ACS APPLIED MATERIALS & INTERFACES

Research Article

Cite This: *ACS Appl. Mater. Interfaces* 2018, 10, 10860−10869

www.acsami.org

Shedding Light on the Oxygen Reduction Reaction Mechanism in Ether-Based Electrolyte Solutions: A Study Using Operando UV−Vis Spectroscopy

Daniel Hirshberg,[†] Daniel Sharon,[†] Michal Afri,[†] Ronit Lavi,[†] Aryeh A. Frimer,[†] Noa Metoki,[‡] Noam Eliaz,[‡] Won-jin Kwak,[§] Yang-Kook Sun,[§] and Doron Aurbach*,[†]

[†]Department of Chemistry and BINA (BIU Institute of Nanotechnology and Advanced Materials), Bar Ilan University, Ramat-Gan 5290002, Israel

[‡]Department of Materials Science and Engineering, Tel Aviv University, Tel Aviv 6997801, Israel

[§]Department of Energy Engineering, Hanyang University, Seoul 133-791, Republic of Korea

Supporting Information

ABSTRACT: Using UV−vis spectroscopy in conjunction with various electrochemical techniques, we have developed a new effective operando methodology for investigating the oxygen reduction reactions (ORRs) and their mechanisms in nonaqueous solutions. We can follow the in situ formation and presence of superoxide moieties during ORR as a function of solvent, cations, anions, and additives in the solution. Thus, using operando UV−vis spectroscopy, we found evidence for the formation of superoxide radical anions during oxygen reduction in LiTFSI/diglyme electrolyte solutions. Nitro blue tetrazolium (NBT) was used to indicate the presence of superoxide moieties based on its unique spectral response. Indeed, the spectral response of NBT containing solutions undergoing ORR could provide a direct indication for the level of association of the Li cations with the electrolyte anions.

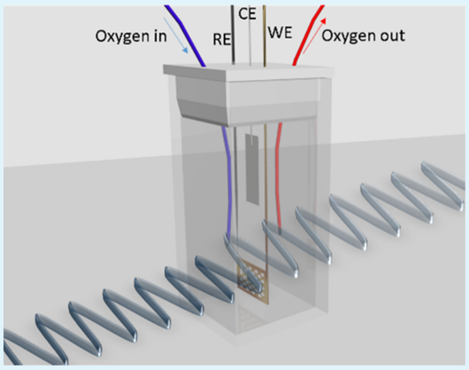

KEYWORDS: *UV−vis spectroscopy, oxygen reduction reactions (ORRs), LiTFSI/diglyme electrolyte solutions, Li-polymer batteries, cyclic voltammetry (CV) curves*

1. INTRODUCTION

Advances in handheld electronic devices require batteries with ever-increasing power and energy density to support the improving levels of sophistication. For now, Li-ion rechargeable batteries are able to furnish the required power and energy; however, there is a rapidly growing gap between supply and demand. A breakthrough is thus imperative if the field of electromobility is to become a practical reality in the near future. More substantial energy and power densities are required to enable vehicles to attain high-speed travel with a significant mileage between charges.

The field of Li-air batteries[1] was born in 1996 when Abraham et al. introduced oxygen into Li-polymer batteries. Over the past two decades, much research has been carried out, and considerable progress has taken place,[2−22] but a commercial Li-air battery is still far beyond reach. This is because of many challenges—not the least being the need to use pure oxygen to avoid contamination by water and CO_2.[5] Hence, only Li-(pure)−O_2 systems can be truly considered, yet many problems still impede their smooth operation.

It has been shown that the main discharge product of Li−O_2 batteries is indeed lithium peroxide,[5,10,15,17−20,22−24] and several mechanisms have been proposed for its formation.[10,23,25−34] To evaluate the various proposals, we must elucidate the basic mechanism of the oxygen reduction, specifically in glyme-based electrolyte solutions. This is because considerable research has shown that these ethereal solvents are the most suitable for Li−O_2 rechargeable batteries.[35,8,12,19,22−24,36]

In the present study, we harnessed UV−vis spectroscopy to shed more light on the mode of oxygen reduction in ether-based electrolyte solutions in the presence of lithium ions. We do not deal here with the two important problems facing Li−O_2 batteries—high over-voltages and side reactions—but rather with the main oxygen reduction reaction (ORR) that occurs in Li−O_2 cells.

2. RESULTS AND DISCUSSION

The spectro-electrochemical cell used for these studies is presented in Figure S1. The cyclic voltammetry (CV) curves in Figures S2−S4, related to $TBAClO_4$ and NaTF solutions in dimethyl sulfoxide (DMSO) and tetrabutylammonium bis-trifluoromethanesulfonimidate (TBA-TFSI)/diglyme solution, respectively, indicate that in a given electrochemical window, oxygen is reduced reversibly to superoxide (O_2^-). This is

Received: December 21, 2017
Accepted: March 7, 2018
Published: March 7, 2018

indicated by a pair of corresponding peaks around 2 V vs Li. Pushing the potential in these solutions to very low values renders the process less reversible because it forces the formation of peroxide moieties. In turn, with the Li-salt solutions in diglyme, we could not detect the typical electrochemical response of reversible formation of superoxide (see further explanations in the SI).

Ethereal electrolyte solutions were found to be the most suitable for ORR, due to their high cathodic stability under the harsh basic/reducing conditions in Li−O_2 cells.[12,22,36,37] The big question that we have tried to answer is whether or not the mechanism for lithium peroxide formation goes through a one-electron transfer to form superoxide moieties as intermediates, or through a two-electron process to directly form lithium peroxide.

UV−vis spectroscopy was used to identify superoxide in some specific solutions based on its unique absorption peak at ca. 270 nm.[38,39] The general assumption today is that ether solvents have a low donor number (DN) and, hence, are unable to solvate Li-superoxide moieties.[22] DMSO, on the other hand, has a high DN and is, therefore, able to solvate the Li-superoxide species. Contributing to the high reactivity of the superoxide ion is the presence of the highly electrophilic Li cations. The latter are very strong Lewis acids; hence, their coupling with superoxide anion radicals immediately forms the LiO_2 species. In fact, solvents with high donor number, like DMSO, stabilize Li-superoxide by interacting with the Li cations, which attenuates their strong electrophilicity.

Before performing any operando experiments, we tried to ascertain the location of the UV−vis absorption peaks of superoxide in diglyme. Figure 1 shows the UV−vis spectra of KO_2 dissolved in diglyme, which contained 0.3 M of recrystallized 18-crown-6 ether.[40] The presence of the crown ether species in diglyme was essential for dissolving KO_2. Solutions with several concentration of KO_2 were prepared and their UV−vis spectra are presented in Figure 1.

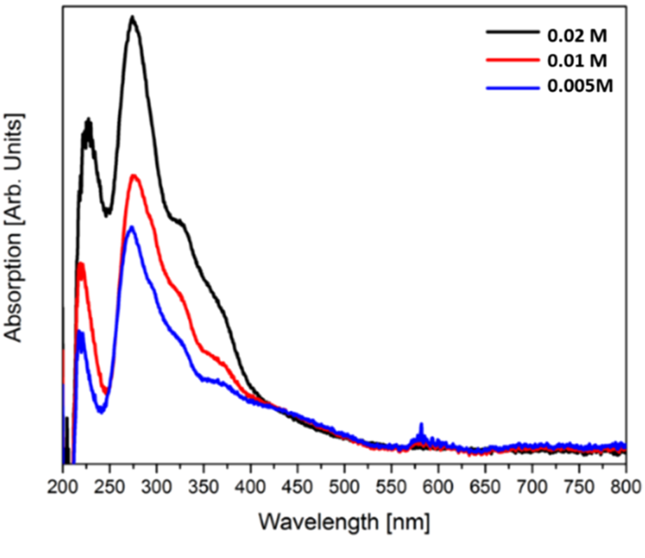

Figure 1. Observed spectrum of KO_2 dissolved in diglyme at different concentrations (indicated).

The spectrum of KO_2 in diglyme reveals a complex behavior, showing several peaks ranging from 200 to 400 nm over a large concentration range. We see that the peaks at wavelengths lower than 300 nm do not directly obey Beer Lambert's law. The complex behavior is not unexpected because this solution is more complex than a regular electrolyte solution. The main issue is the solvation of KO_2, which is more likely to form contact pairs in the solution, rather than to have an ideal charge separation. The main take-home lesson from Figure 1 is that we can clearly observe the presence of superoxide in ether-based electrolyte solutions by UV−vis spectroscopy.

To overcome the interference from oxygen absorption in the spectro-electrochemical measurements, we flushed the cells before each measurement with pure oxygen for 5 min. We then closed the valves and waited for the spectroscopic signal to become stable before taking it as our reference (about 30 min). We started the galvanostatic mode (as a first step) only after clear stabilization of the spectral signal of the cell. Cathodic polarization of the cells with TBA or Na salts solutions in DMSO under oxygen atmosphere indeed showed a clear response that can be assigned to superoxide formation and presence.

Figure 2a shows the full UV−vis spectra of the cell presented in Figure S1 containing 0.2 M TBA/ClO_4 DMSO electrolyte solution, under oxygen atmosphere at rest and upon cathodic polarization, as indicated. During discharge, we observe the formation of three peaks: one peak at ca. 257 nm and two additional peaks in the 300−330 nm range. Both absorption ranges were used to demonstrate operando measurements of superoxide formation and presence during ORR in DMSO and diglyme solutions. In Figure 1, we observe that the peak at 310 nm has no concentration-dependent shift and obeys the Beer−Lambert law. It is important to note that oxygen has an absorption peak in the low region 220−240 nm, which can only slightly affect the measurements at 257 nm.

Figure 2b clearly shows that the spectroscopic signal at 310 nm assigned to superoxide starts to increase only after the galvanostatic cathodic polarization starts. Another thing to note is that the intensity of the absorbance does not decrease after the end of polarization, which means that stable superoxide moieties are formed electrochemically in these solutions. In parallel experiments, cells containing 0.2 M $TBAClO_4$ in DMSO solution under oxygen atmosphere were placed in the spectrometer that was adjusted to measure at 257 nm and operated by repeated cyclic voltammetry in the potential ranges at which superoxide is reversibly formed and decomposes (see Figure S2). Hence, the intensity of the absorbance thus measured should fluctuate according to the voltammetric operation and the formation/disappearance of superoxide species in the cell. Typical results of these experiments are presented in Figure 2c.

Both the periodic potential changes and the spectral response are presented in this figure. A typical steady-state CV is shown in the inset to Figure 2c. The results thus presented show that the operando setup reported and described herein can successfully detect the presence of the superoxide formed electrochemically in the electrolyte solutions in which it is formed during ORR. Thereby, this methodology can be developed further as an important mechanistic tool. Now that we know that the operando setup is operational, we can investigate more complicated systems.

Figure 3 presents the full UV−vis spectra of the cell used herein, containing 0.2 M NaTF/DMSO solution under oxygen atmosphere, at rest and after different periods of time during cathodic polarization during which ORR takes place. The spectra clearly show the appearance of broad peaks in the 300 nm region, which intensify as the cell's polarization progresses.

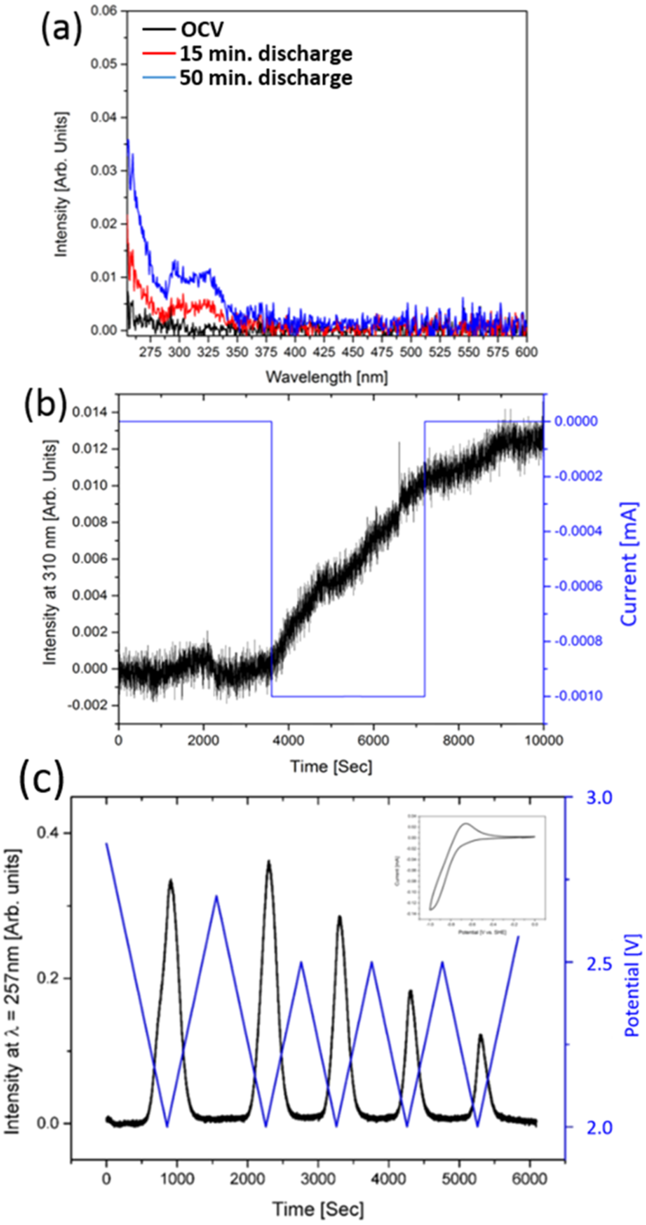

Figure 2. (a) Full UV−vis spectra of the cell used for these studies, containing $TBAClO_4$/DMSO solution under oxygen atmosphere during rest and discharge processes. (b) An operando spectroelectrochemical measurement at rest and during cathodic polarization in which ORR takes place (see the relevant potential range in Figure S2). The spectrometer was adjusted to detect absorption at 310 nm, in which superoxide moieties are spectrally active. The voltage was measured vs a Pt wire pseudo-reference electrode. (c) UV spectroscopic response to cyclic voltammetry of the cell used for this study, containing 0.2 M $TBAClO_4$/DMSO solution under oxygen. The inset shows a steady-state CV at 1 mV s^{-1}. The voltage was measured vs Pt wire pseudo-reference electrode.

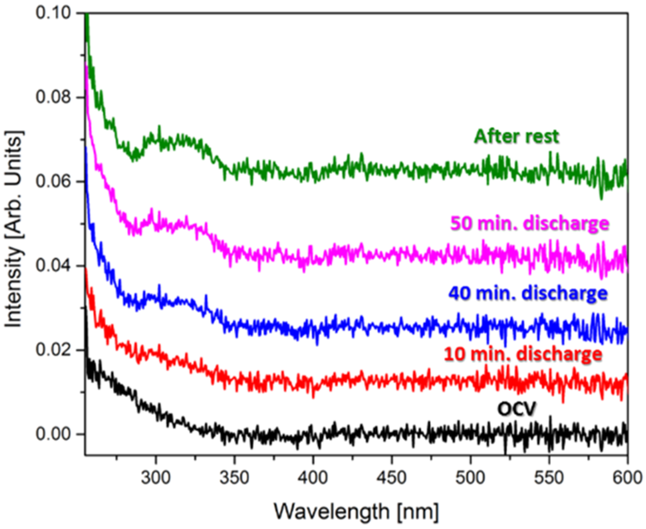

Figure 3. Full UV−vis spectra of the electrochemical cell containing 0.2 M NaTf/DMSO solution under oxygen atmosphere—at rest and during cathodic polarization in which ORR takes place.

We ascribe these broad peaks to the formation of Na-superoxide moieties, which can be well stabilized in DMSO. The signal-to-noise ratio of these measurements is low due to the nature of the superoxide moieties and their relatively low concentration. Improving the sensitivity of these measurements is the goal of further studies. In this work, we intend to show that the methodology works and provides indication for the superoxide formation despite the low signal-to-noise ratios thus obtained.

These results in DMSO are encouraging. The spectral studies of KO_2 solutions and the cells containing DMSO solutions of TBA and Na salts during ORR are coherent. They demonstrate the feasibility of detecting superoxide moieties once they are formed, and reach the necessary concentration for detection by UV−vis spectroscopy. An interesting point indicated by the results presented in Figure 3 is the apparent stability of the Na-superoxide species when polarization is stopped and the cell returns to its OCV.

The next step is to use this methodology for understanding the more complicated ORR in ethereal solutions, which seem to be the most suitable electrolyte systems for Li−oxygen batteries. Diglyme solutions were selected for the present study because we discovered previously that among the ethereal solvents, diglyme is the best for Li−oxygen batteries.[12,15,41] In all ethereal solutions (including diglyme), stabilization of superoxide moieties is much less feasible due to the low donor properties of these solvents. Hence, it is not clear at all if ORR in any diglyme solution forms detectable superoxide moieties. To answer this question, we also used the electron paramagnetic resonance (EPR) spectroscopy, which is capable of detecting superoxide in the solution.

In fact, we tried to develop an operando methodology for Li−oxygen cells using EPR spectroscopy, but found it very unreliable for in situ measurements of these systems. We, therefore, carried out EPR measurements only in an ex situ mode.

Figure 4 shows the EPR spectra of KO_2 dissolved in diglyme and that of 0.2 M TBA-TFSI/diglyme solution that was taken from the electrochemical cell (Figure S1) after ORR. Both spectra show clear EPR signals that we naturally assign to the superoxide species. Not surprisingly, the spectra are not identical due to concentration and cation effects. However, we conclude that superoxide is indeed formed in diglyme solutions and remains stable, at least when "soft" Lewis acid cations like TBA^+ are involved.

The next step is to examine the TBA-TFSI/diglyme solutions in the electrochemical cell during ORR operando by UV−vis

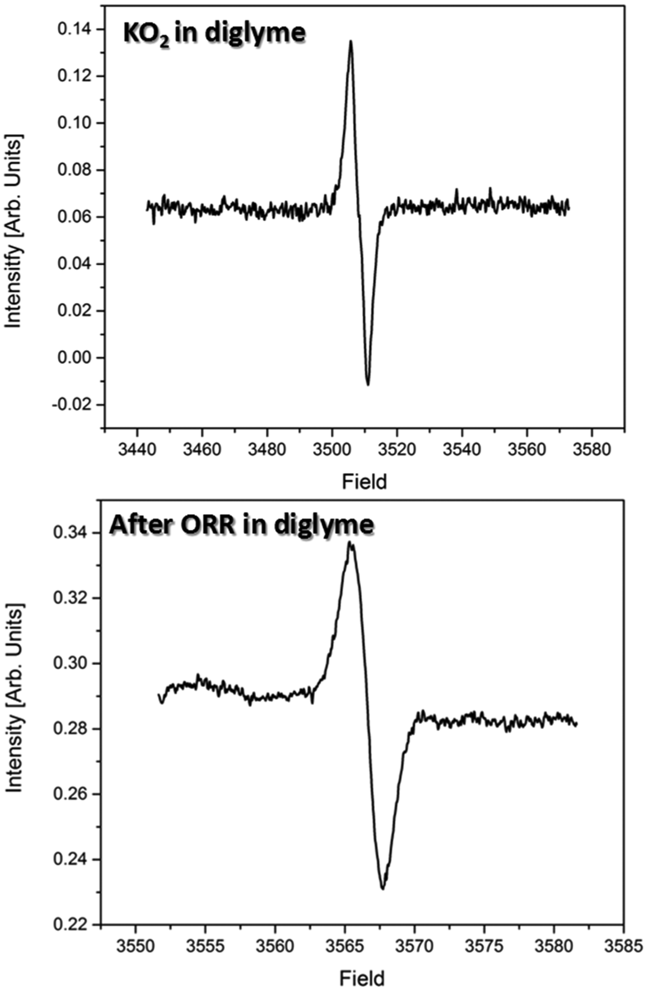

Figure 4. EPR spectra of KO_2 in diglyme and of 0.2 M TBA-TFSI/diglyme solution, taken from the electrochemical cell (Figure S1) after ORR.

spectroscopy. In particular, we compare relevant spectra from these in situ measurements to spectra measured ex situ (out of the cell) with the same solutions after undergoing ORR. Figure 5 shows the spectra of operando and ex situ UV−vis measurements of 0.2 M TBA-TFSI/diglyme solutions during and after ORR, respectively. We note that the two spectra in Figure 5 are overall similar, though the spectrum measured ex situ is much less noisy. They both show broad absorption signals in the 260−315 nm range that can be assigned to superoxide species based on the comparison to Figures 1−3.

The next step is operando studies of Li-salt solutions in diglyme during ORR, using UV−vis spectroscopy. In all Li-salt solutions in ethereal solutions, Li-peroxide is the ultimate final product of oxygen reduction. In previous work, we showed that the nature of the Li salt very strongly affects the deposition mechanism of Li-peroxide in ethereal solutions.[28] The key factor is the level of association between the Li cations and the salt anions in solution. As the extent of association increases, the Li cations become more stable and their electrophilicity drops. Consequently, the superoxide or peroxide moieties are stabilized in the solution (by the Li cations) and Li-peroxide precipitates via a top−down mechanism (thus forming thick deposits).

When the Li salts do not form associated ions in the solutions, the Li cations act as strong Lewis acids and the

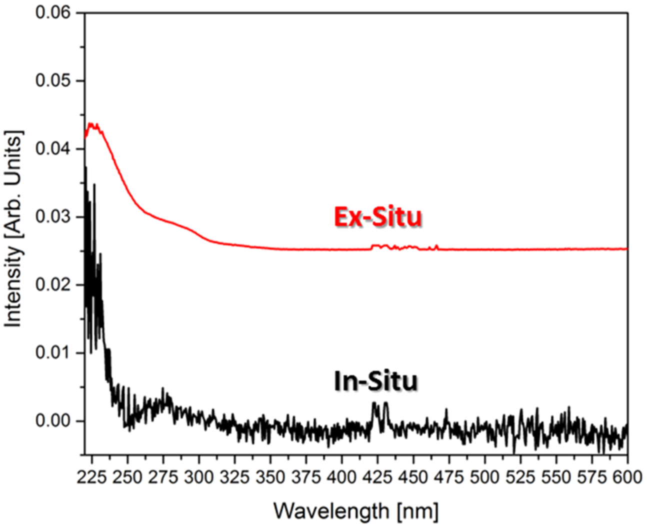

Figure 5. Comparison between ex situ UV−vis spectra measured ex situ and in situ with 0.2 M TBA-TFSI/diglyme electrolyte solutions. The lower spectrum was measured in the electrochemical cell during ORR. The upper one was run with a solution taken from the cell after it underwent ORR.

interactions between the Li ions and the reduced oxygen species occur on the electrode surface. This, in turn, leads to a bottom−up mechanism of Li-peroxide precipitation (in thin dense layers).[28]

The operando measurements described herein may be affected strongly by the nature of the Li salts in diglyme solutions. With Li salts that form associated ions in the solutions (stabilized Li cations), we may be able to detect superoxide intermediates formed during ORR (due to the stabilization effect).

Figure 6 shows the representative results of operando experiments with LiTFSI, LiTF, and $LiNO_3$ solutions in diglyme as indicated. Upon studying these solutions, the cells described in Figure S1 were used with Li wire reference electrodes. The voltammetric behavior of these solutions, which are very complicated, is provided in Figures S5−S7, respectively. The assignment of these CV responses to certain processes is very problematic. Thereby, exploring these solutions with spectro-electrochemical measurements may be crucially important for understanding the oxygen reduction processes occurring in them. The left panels of Figure 6 show the potential profiles of the experiments (galvanostatic operation), in which the points at which spectra were measured are marked. The right column shows various spectra—as indicated. In terms of Li-association, NO_3^- is an highly associated anion to Li^+, $TSFI^-$ is the least associated anion, and $CF_3SO_2O^-$ (TF) shows an intermediate response. Interestingly (and in line with our expectation), the UV−vis spectra related to LiTFSI solutions (panels a and b) do not show any signal that can be assigned to superoxide.

With LiTF solutions, only the spectra measured after 70 min of discharge (ORR) could show a small signal around 300 nm.

On the other hand, all the spectra measured during ORR with the cell containing $LiNO_3$ solution (the most associated Li salt) showed a broad pronounced absorption around 300 nm, which can be assigned to superoxide moieties. The flat voltage profile (around 2.4 V vs Li) measured with this solution (panel e) reflects the precipitation of Li-peroxide at high capacity. This is explained by the top−down mechanism of the Li-peroxide

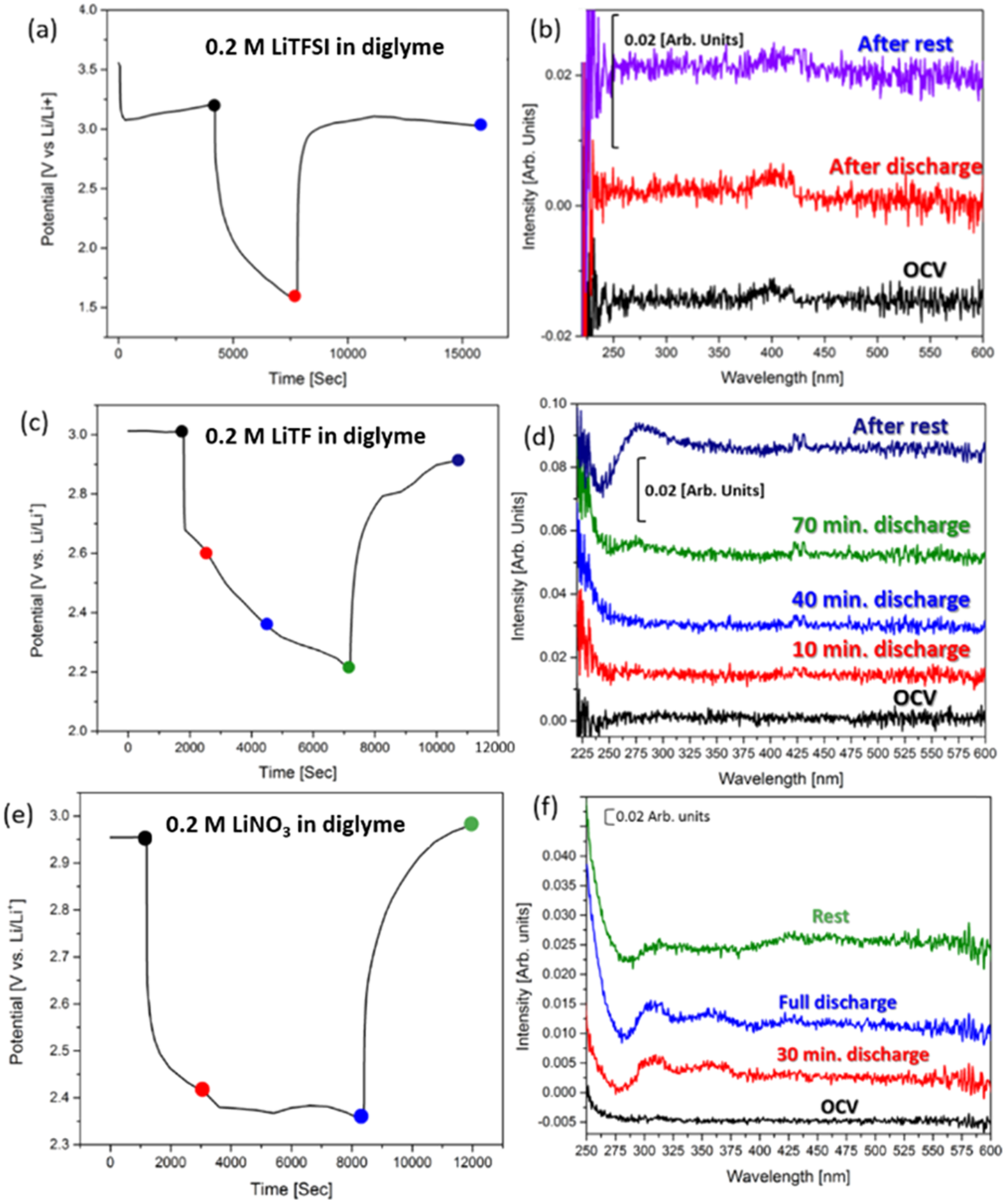

Figure 6. UV−vis spectra (right panels) and voltage profiles (left panels) of the electrochemical cell (Figure S1) loaded with diglyme solutions of 0.2 M LiTFSI (a, b), LiTF (c, d), and $LiNO_3$ (e, f) as indicated under oxygen atmosphere. Galvanostatic operation, starting with OCV ending at rest (no current). The points at which the spectra were measured are marked on the voltage profiles. The voltages measured using Pt quasi-reference electrodes were translated to the Li scale.

formation via reaction of stabilized superoxide moieties accumulating in the solution. Hence, Figure 6 presents a very logical picture of the ORR in diglyme solutions with different Li^+ salts. As the association of the Li cations with the anions increases, the voltage profiles show a higher specific capacity of the ORR (before the potentials drop too low), and the superoxide related UV−vis peaks become more detectable.

The question, however, remains: If we do not see any spectroscopic signal for superoxide with LiTFSI/diglyme solutions, does this mean that superoxide is not formed in

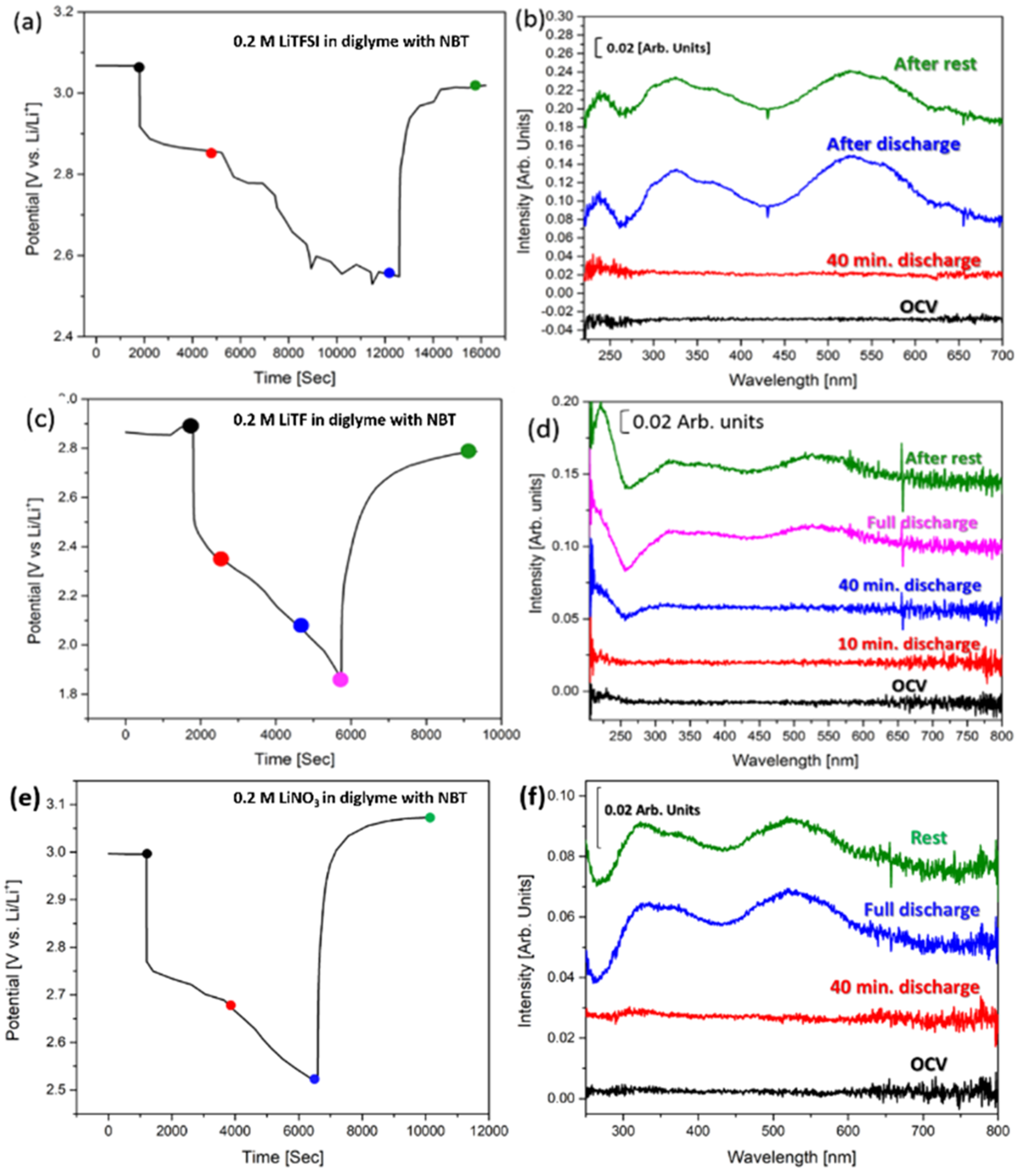

Figure 7. UV–vis spectra (right-hand charts) and voltage profiles (to the left) obtained via operando experiments with 0.2 M Li-salt/diglyme solutions containing NBT: (a, b) LiTFSI, (c, d) LiTF, and (e, f) $LiNO_3$ under oxygen atmosphere.

them at all? To enhance the detectability of superoxide species in the Li-salt solutions in diglyme, we used nitro blue tetrazolium (NBT) as a superoxide-trapping sensor. The molecular structure of NBT and its superoxide trapping reactions in aqueous solutions are illustrated in Figure S8. NBT is well known as a detector of the presence of superoxide in biological systems (aqueous solutions) by changing the color of the solution (and hence its UV–vis absorption). If the superoxide is formed in LiTFSI/ethereal solutions, the use of NBT indicator can assist in its detection provided that the rate of the NBT–superoxide reaction is several times faster than a possible reaction of superoxide (formed by ORR) with Li^+ cations or the solvent molecules. Note that the superoxide-trapping reaction of NBT in protic media must involve reactions with protons, as presented in Figure S8. We suggest that NBT can be used in nonaqueous Li-salt solutions as well, with Li cations interacting with NBT in a similar manner as protons do in aqueous media.

DOI: 10.1021/acsami.7b18376
ACS Appl. Mater. Interfaces 2018, 10, 10860–10869

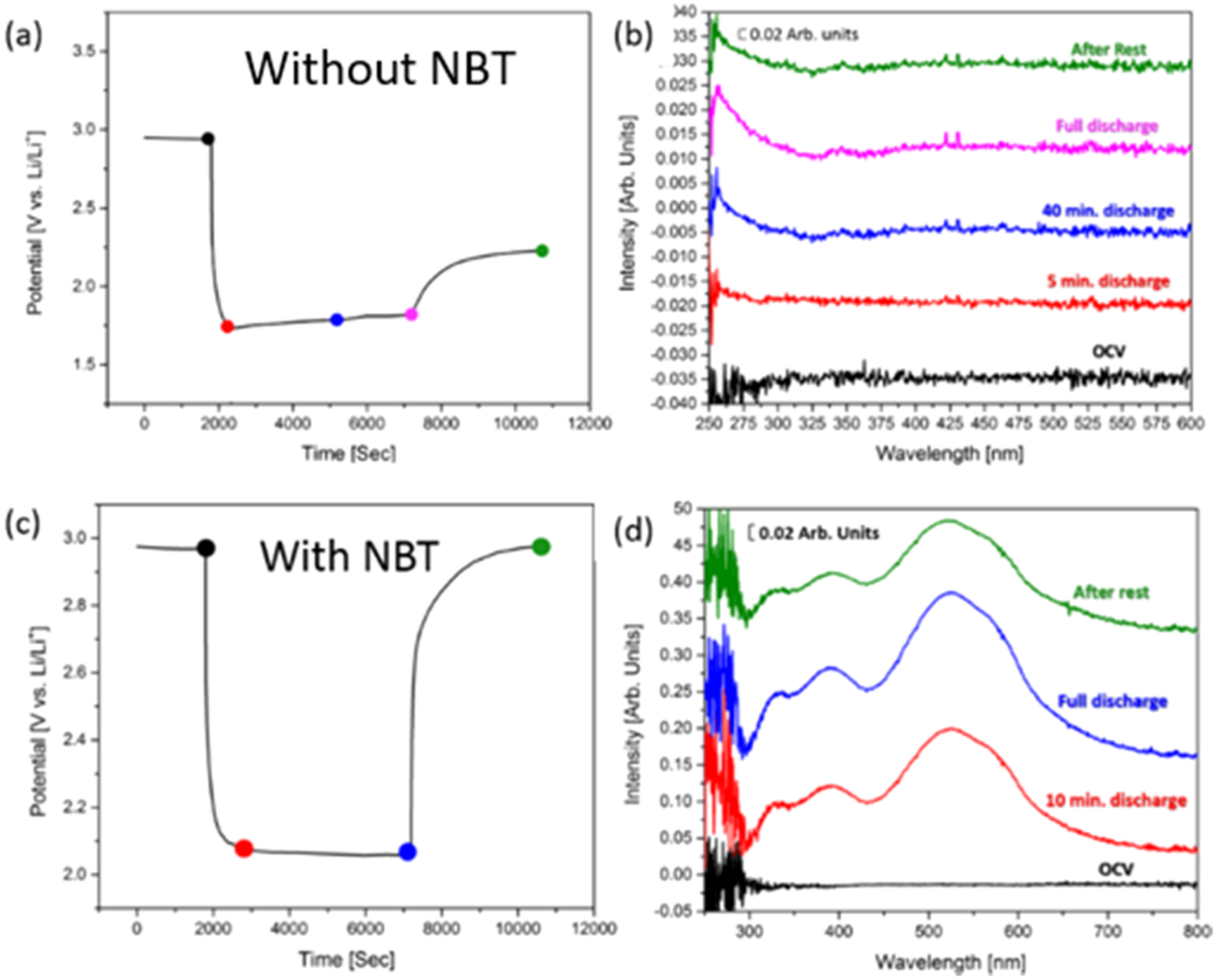

Figure 8. Voltage profiles (galvanostatic operation) and full spectra of cells with 0.2 M LiTFSI/DMSO: (a, b) without NBT and (c, d) with NBT-measured during operando experiments under oxygen atmosphere.

Before our work, we are unaware of any report of NBT being used in ethereal solutions. Therefore, we verified that NBT dissolves in diglyme solutions and reacts therein with superoxide species. We observed that about 1 mg NBT in 10 mL of diglyme gives a clear solution, so this concentration was used throughout the subsequent experiments. Figure S10 shows the UV−vis spectra of NBT/diglyme, 0.01 M KO_2/diglyme, and 0.01 M KO_2/diglyme/NBT solutions.

We observe in Figure S10 that for NBT with KO_2 in diglyme, an extra peak is formed in the 530 nm region. This correlates to previous studies.[42] However, before using NBT in our operando setup, we had to ensure that it reacts with the ORR products and that it is specific to superoxide and not to peroxide.

When NBT is added to a TBA-TFSI/diglyme solution after the ORR, a distinct color change is observed (Figure S11b); the color change is much more pronounced when NBT is added to a KO_2/diglyme solution (Figure S11c). This is expected because in that solution, there is 0.01 M of KO_2 compared to about 0.005 M of superoxide in the solution after ORR (calculated based on the capacity of the electrochemical process).

The most important result shown in Figure S11 is the fact that there is no color change when adding NBT to a solution containing Li_2O_2. The results presented in Figures S10 and S11 mean that NBT is reactive with the ORR products in diglyme solutions, but specifically with superoxide and not with peroxides.

The UV−vis spectra measured with a TBA-TFSI/diglyme solution after ORR and with Li_2O_2/diglyme solution after NBT was added to them, are presented in Figure S12.

Figure S12 reveals that when NBT is added to a solution of Li_2O_2 in diglyme, there is no UV−vis peak in the 500 nm region. The Li_2O_2 solution spectrum somewhat resembles that of the superoxide in the lower portion of the spectrum, but the 300 nm region has no peaks. In turn, the TBA-TFSI/diglyme solution after ORR, to which NBT was added, shows a very clear, broad UV−vis at around 500−550 nm. This confirms that the reduction of oxygen in TBA-TFSI/diglyme solution forms detectable superoxide moieties despite the low donor properties of this ethereal solvent. These results also show that the UV−vis spectroscopy can serve as an important analytical tool for following oxygen reduction processes in ethereal solutions.

Before NBT can be added to operando experimental solutions, it is necessary to make sure that NBT itself is not electrochemically reduced. Figure S9 shows the electrochemical response of the cell (Figure S1) containing 0.2 M LiTFSI/diglyme/NBT under argon and oxygen atmospheres. It compares the voltage profiles in galvanostatic experiments. As clearly demonstrated in this figure, without oxygen, there is no reaction, whereas under oxygen, the voltage profile reflects the usual and expected ORR. This indicates that NBT is not intrinsically electrochemically reactive, and it may be possible to add NBT to these solutions for operando experiments. Figure 7 presents a full set of operando experiments with 0.2 M LiTFSI, LiTF, and $LiNO_3$ solutions in diglyme which contained NBT.

In Figure 7, we observe that the presence of NBT has an effect on the voltage profiles of all the electrolyte solutions. The most affected is the behavior of the LiTFSI solution, whose voltage profile in the presence of NBT resembles that of $LiNO_3$ solution without NBT (Figure 6). With $LiNO_3$ solution, the spectrum below 250 nm is very noisy because NO_3^- ions are absorbed in this region. As a result, the spectral response of this solution is shown in Figure 7 at wavelengths >250 nm. As we mentioned earlier, if the ORR, when LiTFSI is the electrolyte, forms a superoxide anion radical as an intermediate, the use of NBT proves to be an excellent way of detecting it. Figure S10 shows the results of a typical operando experiment with the cell charged in the LiTFSI/diglyme solution containing NBT. The cell was operated in galvanostatic mode and the voltage profile is seen in the figure. The spectrometer was adjusted to absorb at 530 nm, which is the absorption seen when the solution contains NBT, which reacts with the superoxide species. The spectral response follows the ORR very closely, as is clearly seen in Figure S10. It seems clear that ORR, in all the three diglyme/Li-salt solutions containing NBT, produces superoxide moieties. Further proof is required to prove that ORR in these Li-salt/diglyme solutions really produces stable super-oxide moieties as intermediates, in the overall reaction that forms Li-peroxide as the end product. It is likely that the presence of NBT channels the ORR, which produces stabilized superoxide intermediates due to its interaction with this radical anion (Figure S8). Indeed, comparing the voltage profiles (Figures 6 and 7) and the CV response (Figures S5 and S14) of LiTFSI/glyme solutions with and without NBT (respectively) reveals a pronounced effect of the presence of NBT. There is a flat plateau around 2.5 V (Figure S11a) corresponding to a more pronounced redox activity in the range of 2−3 V in the cyclic voltammetric response. Hence, we suspect that NBT may not be just an indicator of the presence of superoxide in Li-salt/diglyme solutions but also a promoter of its formation. This it does by catching the superoxide at the instant that it is formed during ORR. We visually see the strongest color change—and the most intense 500−550 nm broad peak formation—during ORR with solutions containing LiTFSI (compared to LiTF and $LiNO_3$ solutions), which requires explanation. LiTFSI is one of the most dissociated Li salts in ethereal solvents, and, hence, the Li cations in LiTFSI/glyme solutions should be relatively free. Considering the NBT−superoxide interaction mechanism presented in Figure S8, in aqueous media, the protons are required to complete the reaction. In the dry diglyme solutions, there are no protons available. However, Li^+ ions like protons serve as strong Lewis acid species. We, therefore, hypothesize that Li^+ cations can take the place of protons in completing the NBT−superoxide reactions. Hence, when the Li^+ cations in solution are free, i.e., unassociated with the anions, the effect of NBT may be more pronounced.

Another interesting case is the use of LiTFSI in DMSO as the electrolyte solution. Because DMSO is a solvent with a high donor number that can stabilize Li cations, it may be possible to follow superoxide formation in this solution during ORR, even without the presence of NBT. Figure 8 shows the operando studies of ORR with 0.2 M LiTFSI/DMSO solution.

When DMSO is the solvent, ORR in a LiTFSI solution seems to produce superoxide species as relatively stable intermediates. This can be concluded from the spectra in Figure 8b that shows an increasing absorption band at a wavelength <300 nm as the ORR progresses. When the solution contains NBT, the oxygen reduction occurs at higher potentials. In addition, the color change and the intensity of the broad peaks around 500 nm as ORR proceeds is much stronger compared to the experiments with LiTFSI/diglyme solutions. The change in the ORR potential due to the presence of NBT may suggest that it affects the reaction and the possible formation of superoxide. The spectral signals clearly suggest that the high donor properties of DMSO allow the formation of stable superoxide intermediates without the involvement of complexation with NBT. When the latter is present in Li-salts/DMSO solutions, its effect in promoting superoxide formation and stabilization is amplified as compared to the case of ethereal solutions.

3. CONCLUSIONS

In this work, we have developed a new methodology for studying the mechanisms of oxygen reduction reactions (ORR) in nonaqueous solutions using operando UV−vis spectroscopy, in conjunction with electrochemical measurements. A highly important mechanistic question related to ORR arises: Are superoxide species involved as intermediates in these processes? This is critically important information because their formation and stabilization may strongly affect the nature of the end products (composition, morphology, and maximal capacity), reversibility, and possible detrimental side reactions. The formation of superoxide and its stabilization during ORR depends on the nature of the solvent (donor number), cation (TBA^+, Na^+, Li^+), and anion (the level of association with the cation in solution). In this work, we tested two types of solvents (DMSO and diglyme), the above three types of cations, and three types of anions ($TFSI^-$, TF^-, and NO_3^-). We demonstrate that superoxide species formed in both DMSO and diglyme solutions (different cations and anions) can be detected by UV−vis spectroscopy and, hence, it is possible to conduct operando studies of superoxide formation and stabilization during ORR in these systems. We also demonstrate that NBT can be used as an effective marker for superoxide species formed during ORR, which amplifies their detectability by UV−vis spectroscopy. However, the presence of NBT in Li-salt solutions may change the true mechanism of ORR in them because NBT stabilizes the superoxide moieties upon reacting with them. Hence, we may detect stable superoxide species formed upon ORR in Li-salt solution only because they contain NBT. Thus, to develop the usefulness of the methodology presented herein, it may be necessary to modify the operation protocol: the electrochemical processes should be carried out in NBT-free solutions. For a spectroscopic measurement, NBT should be injected into the cell, whereas the electrochemical stimulation is halted. The results presented herein in terms of authentic detection of superoxide species (no NBT in solution during the electrochemical process) are consistent with many previous findings about the effect of solution composition (solvent, cation, and anion). Further efforts are required to improve the signal-to-noise ratio of the UV−vis measurements. In addition, cells whose structure is closer to that of batteries should be developed following subsequent steps. We believe that the present results mark a breakthrough in the analytical capability of exploring Li and Na oxygen batteries.

4. MATERIALS AND METHODS

4.1. Materials. High-purity diglyme (diethylene glycol dimethyl ether; 99.99% anhydrous) and DMSO (dimethyl sulfoxide anhydrous; ≥99.9%) were obtained from Sigma-Aldrich and dried over 4 Å molecular sieves. The electrolytes $LiN(SO_2CF3)_2$ (LiTFSI, 99.95% anhydrous), tetrabutylammonium bis-trifluoromethanesulfonimidate (TBA-TFSI ≥99%), tetrabutylammonium perchlorate ($TBA-ClO_4$ ≥99%), lithium trifluoromethanesulfonate (LiTF 99.995%), and anhydrous lithium nitrate (99.999%) were also purchased from Sigma-Aldrich. All salts were exposed exclusively to argon atmosphere and dried before use under high vacuum (<1 mTorr) as follows: LiTFSI (72 h, 150 °C), $LiNO_3$ (72 h, 150 °C), TBA-TFSI (72 h, 100 °C), and $TBA-ClO_4$ (72 h, 100 °C). 18-Crown-6 ether (99.5%, Sigma-Aldrich) was dried by recrystallization from dry acetonitrile (99.95% anhydrous, Sigma-Aldrich). The nitro blue tetrazolium (NBT) chloride salt was purchased from Sigma-Aldrich and stored at 4 °C before use. Potassium superoxide (KO_2) was purchased from Sigma-Aldrich and used as received.

Pure Pt metal gauze 1042 mesh cm^{-1} was used as the working electrode, whereas pure Pt metal sheet was used as the counter electrode, and pure Pt wire was used as a quasi-reference electrode in several measurements (as indicated in the relevant panels). For many of the measurements, especially with Li-salt solutions, the potentials in the charts were plotted in the Li^+/Li scale. In all of the solutions, the Pt pseudo-reference electrode was calibrated vs Li metal reference electrode and the stability of its potential was confirmed. The platinum parts for this work were purchased from Holland Moran (Israel).

4.2. Cell Fabrication. The operando cells consisted of a quartz cuvette (Starna Scientific), sealed using a Teflon screwcap with all three electrodes inside. All cell assemblies were carried out in an argon-filled glovebox (water and oxygen contents were less than 1 ppm). After assembly, the operando cells were connected to a pure oxygen cylinder (99.999%) and flushed and kept under positive pressure under a flow of oxygen for the entire duration of the experiment. A cell and the illustration of its spectral measurements are described in Figure S1. Although it is a single compartment cell, the light beam is incident on the cell through the working electrode (cathode), and the distance between the electrodes in the stationary operations may avoid any significant mixing between the cathode and anode sides. As a result, we assumed that the spectral measurements reflect the results of the reactions on the cathode only.

4.3. Electrochemical and Spectroscopic Measurements. We carried out galvanostatic and cyclic voltammetry measurements employing various solutions including 0.1 M $TBAClO_4$, 1 M LiTFSI, and 1 M $LiNO_3$ in diglyme and 0.1 M TBA-TFSI with and without addition of ca. 1 mg of NBT. The results of periodic cyclic voltammetry measurements of $TBAClO_4$ and NaTF solutions in DMSO, TBA-TFSI, LiTFSI, LiTF, and $LiNO_3$ solutions in diglyme in the cells used herein under oxygen atmosphere are presented in Figures S2−S7, respectively. In the experiments upon which Figures S2−S7 are based, the voltage windows were opened progressively from cycle to cycle to follow the potential effect on the ORR and OER in these systems. The solvents were stored over 4 Å molecular sieves in an argon-filled glovebox (final water content <10 ppm, determined with Mettler-Toledo Karl-Fischer titration). The electrochemical measurements were performed using computerized potentiostat−galvanostat VMP3 systems from Bio-Logic (France). Typical UV−vis measurements were carried out with an AvaSpec-ULS2048 spectrophotometer with a deuterium lamp from Avantes (The Netherlands).

4.4. EPR Measurements. The X-band EPR spectra of the solutions were obtained at room temperature on a Bruker ELEXSYS E500 cw X-band EPR spectrometer equipped with a standard rectangular Bruker EPR cavity (ER 4119 HS). The EPR was operating at a microwave frequency of ca. 9.87 GHz and the spectra were recorded using a microwave power of 20 mW and sampling time of 1 min.

■ ASSOCIATED CONTENT

Supporting Information

The Supporting Information is available free of charge on the ACS Publications website at DOI: 10.1021/acsami.7b18376.

> Schematics of the operando setup; molecular schematic of the NBT molecule; voltage profiles of cells with 0.2 M LiTFSI/diglyme solutions; UV−vis spectra of NBT/diglyme; effect of NBT addition to diglyme; voltage profile (galvanostatic operation) and the intensity (PDF)

■ AUTHOR INFORMATION

Corresponding Author

*E-mail: Doron.Aurbach@biu.ac.il. Tel: +972-3-5318832. Fax: +972-3-5317291.

ORCID

Daniel Hirshberg: 0000-0002-8582-0096
Daniel Sharon: 0000-0002-3385-1536
Yang-Kook Sun: 0000-0002-0117-0170
Doron Aurbach: 0000-0001-8047-9020

Notes

The authors declare no competing financial interest.

■ ACKNOWLEDGMENTS

A.A.F. thanks the Israel Science Foundation (ISF; Grant No. 1469/13) as well as the Ethel and David Resnick Chair in Active Oxygen Chemistry for their kind and generous support. Partial support for this work was obtained by Israel Prime Minister office and the Israel Committee of High Education in the framework of the INREP project.

■ REFERENCES

(1) Abraham, K. M. A Polymer Electrolyte-Based Rechargeable Lithium/Oxygen Battery. *J. Electrochem. Soc.* **1996**, *143*, 1−5.

(2) Viswanathan, V.; Nørskov, J. K.; Speidel, A.; Scheffler, R.; Gowda, S.; Luntz, A. C. Li-O_2 Kinetic Overpotentials: Tafel Plots from Experiment and First-Principles Theory. *J. Phys. Chem. Lett.* **2013**, *4*, 556−560.

(3) Wang, Z.-L.; Xu, D.; Xu, J.-J.; Zhang, X.-B. Oxygen Electrocatalysts in Metal-air Batteries: From Aqueous to Nonaqueous Electrolytes. *Chem. Soc. Rev.* **2014**, *43*, 7746−7786.

(4) Freunberger, S. A.; Chen, Y.; Peng, Z.; Griffin, J. M.; Hardwick, L. J.; Bardé, F.; Novák, P.; Bruce, P. G. Reactions in the Rechargeable Lithium-O_2 Battery with Alkyl Carbonate Electrolytes. *J. Am. Chem. Soc.* **2011**, *133*, 8040−8047.

(5) Xu, W.; Xu, K.; Viswanathan, V. V.; Towne, S. A.; Hardy, J. S.; Xiao, J.; Nie, Z.; Hu, D.; Wang, D.; Zhang, J.-G. Reaction Mechanisms for the Limited Reversibility of Li-O_2 Chemistry in Organic Carbonate Electrolytes. *J. Power Sources* **2011**, *196*, 9631−9639.

(6) Lu, Y.-C.; Gasteiger, H. A.; Shao-Horn, Y. Catalytic Activity Trends of Oxygen Reduction Reaction for Nonaqueous Li-Air Batteries. *J. Am. Chem. Soc.* **2011**, *133*, 19048−19051.

(7) Hassoun, J.; Croce, F.; Armand, M.; Scrosati, B. Investigation of the O_2 Electrochemistry in a Polymer Electrolyte Solid-State Cell. *Angew. Chem., Int. Ed.* **2011**, *50*, 2999−3002.

(8) Black, R.; Oh, S. H.; Lee, J.; Yim, T.; Adams, B.; Nazar, L. F. Screening for Superoxide Reactivity in Li-O_2 Batteries: Effect on Li_2O_2/LiOH Crystallization. *J. Am. Chem. Soc.* **2012**, *134*, 2902−2905.

(9) Zheng, D.; Wang, Q.; Lee, H. S.; Yang, X. Q.; Qu, D. Catalytic Disproportionation of the Superoxide Intermediate from Electrochemical O_2 Reduction in Nonaqueous Electrolytes. *Chem. - Eur. J.* **2013**, *19*, 8679−8683.

(10) Lu, J.; Lee, Y. J.; Luo, X.; Lau, K. C.; Asadi, M.; Wang, H.; Brombosz, S.; Wen, J.; Zhai, D.; Chen, Z.; Miller, D. J.; Jeong, Y. S.; Park, J.; Fang, Z. Z.; Kumar, B.; Salehi-khojin, A.; Sun, Y.; Curtiss, L. A.; Amine, K. A Lithium-oxygen Battery Based on Lithium Superoxide. *Nature* **2016**, 377−382.

(11) Sharon, D.; Hirshberg, D.; Afri, M.; Frimer, A. A.; Noked, M.; Aurbach, D. Aprotic Metal-Oxygen Batteries: Recent Findings and Insights. *J. Solid State Electrochem.* **2017**, 1861−1878.

(12) Sharon, D.; Hirshberg, D.; Afri, M.; Frimer, A. A.; Aurbach, D. The Importance of Solvent Selection in Li-O $_2$ Cells. *Chem. Commun.* **2017**, *53*, 3269−3272.

(13) Li, Z.; Ganapathy, S.; Xu, Y.; Heringa, J. R.; Zhu, Q.; Chen, W.; Wagemaker, M. Understanding the Electrochemical Formation and Decomposition of Li_2O_2 and LiOH with Operando X-Ray Diffraction. *Chem. Mater.* **2017**, 1577−1586.

(14) Suzen, S.; Gurer-Orhan, H.; Saso, L. Detection of Reactive Oxygen and Nitrogen Species by Electron Paramagnetic Resonance (EPR) Technique. *Molecules* **2017**, *22*, No. 181.

(15) Sharon, D.; Hirsberg, D.; Salama, M.; Afri, M.; Frimer, A. A.; Noked, M.; Kwak, W.; Sun, Y. K.; Aurbach, D. Mechanistic Role of Li+ Dissociation Level in Aprotic Li-O_2 Battery. *ACS Appl. Mater. Interfaces* **2016**, *8*, 5300−5307.

(16) Tan, P.; Shyy, W.; Zhao, T. S.; Wei, Z. H.; An, L. Discharge Product Morphology versus Operating Temperature in Non-Aqueous Lithium-Air Batteries. *J. Power Sources* **2015**, *278*, 133−140.

(17) Sharon, D.; Hirsberg, D.; Afri, M.; Chesneau, F.; Lavi, R.; Frimer, A. A.; Sun, Y.-K.; Aurbach, D. Catalytic Behavior of Lithium Nitrate in Li-O_2 Cells. *ACS Appl. Mater. Interfaces* **2015**, *7*, 16590−16600.

(18) Erikson, H.; Sarapuu, A.; Tammeveski, K.; Solla-Gullon, J.; Feliu, J. M. Shape-Dependent Electrocatalysis: Oxygen Reduction on Carbon-Supported Gold Nanoparticles. *ChemElectroChem* **2014**, *1*, 1338−1347.

(19) Galiote, N. A.; de Azevedo, D. C.; Oliveira, O. N.; Huguenin, F. Investigating the Kinetic Mechanisms of the Oxygen Reduction Reaction in a Non-Aqueous Solvent. *J. Phys. Chem. C* **2014**, 21995−22002.

(20) Xia, C.; Waletzko, M.; Chen, L.; Peppler, K.; Klar, P. J.; Janek, J. Evolution of Li_2O_2 Growth and Its Effect on Kinetics of Li-O_2 Batteries. *ACS Appl. Mater. Interfaces* **2014**, *6*, 12083−12092.

(21) Aetukuri, N. B.; McCloskey, B. D.; García, J. M.; Krupp, L. E.; Viswanathan, V.; Luntz, A. C. Solvating Additives Drive Solution-Mediated Electrochemistry and Enhance Toroid Growth in Non-Aqueous Li-O_2 Batteries. *Nat. Chem.* **2015**, *7*, 50−56.

(22) Johnson, L.; Li, C.; Liu, Z.; Chen, Y.; Freunberger, S. A.; Ashok, P. C.; Praveen, B. B.; Dholakia, K.; Tarascon, J.-M.; Bruce, P. G. The Role of LiO_2 Solubility in O_2 Reduction in Aprotic Solvents and Its Consequences for Li-O_2 Batteries. *Nat. Chem.* **2014**, *6*, 1091−1099.

(23) Torres, W.; Mozhzhukhina, N.; Tesio, A. Y.; Calvo, E. J. A Rotating Ring Disk Electrode Study of the Oxygen Reduction Reaction in Lithium Containing Dimethyl Sulfoxide Electrolyte: Role of Superoxide. *J. Electrochem. Soc.* **2014**, *161*, A2204−A2209.

(24) Sharon, D.; Hirsberg, D.; Afri, M.; Garsuch, A.; Frimer, A. A.; Aurbach, D. Reactivity of Amide Based Solutions in Lithium-Oxygen Cells. *J. Phys. Chem. C* **2014**, *118*, 15207−15213.

(25) Schwenke, K. U.; Meini, S.; Wu, X.; Gasteiger, H. A.; Piana, M. Stability of Superoxide Radicals in Glyme Solvents for Non-Aqueous Li-O_2 Battery Electrolytes. *Phys. Chem. Chem. Phys.* **2013**, *15*, 11830.

(26) Ganapathy, S.; Li, Z.; Anastasaki, M. S.; Basak, S.; Miao, X. F.; Goubitz, K.; Zandbergen, H. W.; Mulder, F. M.; Wagemaker, M. Use of Nano Seed Crystals to Control Peroxide Morphology in a Nonaqueous Li-O_2 Battery. *J. Phys. Chem. C* **2016**, *120*, 18421−18427.

(27) Kwabi, D. G.; Bryantsev, V. S.; Batcho, T. P.; Itkis, D. M.; Thompson, C. V.; Shao-Horn, Y. Experimental and Computational Analysis of the Solvent-Dependent O_2/Li^+-O_2- Redox Couple: Standard Potentials, Coupling Strength, and Implications for Lithium-Oxygen Batteries. *Angew. Chem., Int. Ed.* **2016**, *55*, 3129−3134.

(28) Wang, Q.; Zheng, D.; McKinnon, M. E.; Yang, X. Q.; Qu, D. Kinetic Investigation of Catalytic Disproportionation of Superoxide Ions in the Non-Aqueous Electrolyte Used in Li-Air Batteries. *J. Power Sources* **2015**, *274*, 1005−1008.

(29) Ortiz-Vitoriano, N.; Batcho, T. P.; Kwabi, D. G.; Han, B.; Pour, N.; Yao, K. P. C.; Thompson, C. V.; Shao-Horn, Y. Rate-Dependent Nucleation and Growth of NaO_2 in Na-O_2 Batteries. *J. Phys. Chem. Lett.* **2015**, *6*, 2636−2643.

(30) Johnson, L.; Li, C.; Liu, Z.; Chen, Y.; Freunberger, S. A.; Tarascon, J.; Ashok, P. C.; Praveen, B. B.; Dholakia, K.; Bruce, P. G. The role of LiO2 solubility in O2 reduction in aprotic solvents and its consequences for Li−O2 batteries. *Nat. Chem.* **2014**, 1091−1099.

(31) Meini, S.; Solchenbach, S.; Piana, M.; Gasteiger, H. A. The Role of Electrolyte Solvent Stability and Electrolyte Impurities in the Electrooxidation of Li_2O_2 in Li-O_2 Batteries. *J. Electrochem. Soc.* **2014**, *161*, A1306−A1314.

(32) Balaish, M.; Kraytsberg, A.; Ein-Eli, Y. A Critical Review on Lithium-Air Battery Electrolytes. *Phys. Chem. Chem. Phys.* **2014**, *16*, 2801−2822.

(33) Zheng, D.; Wang, Q.; Lee, H.; Yang, X.; Qu, D. Catalytic Disproportionation of the Superoxide Intermediate from Electrochemical O2 Reduction in Nonaqueous Electrolytes. *Chem. - Eur. J.* **2013**, 8679−8683.

(34) Viswanathan, V.; Speidel, A.; Gowda, S.; Luntz, A. C. Li−O2 Kinetic Overpotentials: Tafel Plots from Experiment and First-Principles Theory. *J. Phys. Chem. Lett.* **2013**, 556−560.

(35) Wang, Z.-L.; Xu, D.; Xu, J.-J.; Zhang, X.-B. Oxygen Electrocatalysts in Metal-air Batteries: From Aqueous to Nonaqueous Electrolytes. *Chem. Soc. Rev.* **2014**, *43*, 7746−7786.

(36) Sharon, D.; Afri, M.; Noked, M.; Garsuch, A.; Frimer, A. A.; Aurbach, D. Oxidation of Dimethyl Sulfoxide Solutions by Electrochemical Reduction of Oxygen. *J. Phys. Chem. Lett.* **2013**, *4*, 3115−3119.

(37) Sharon, D.; Etacheri, V.; Garsuch, A.; Afri, M.; Frimer, A. A.; Aurbach, D. On the Challenge of Electrolyte Solutions for Li-Air Batteries: Monitoring Oxygen Reduction and Related Reactions in Polyether Solutions by Spectroscopy and EQCM. *J. Phys. Chem. Lett.* **2013**, *4*, 127−131.

(38) Schwenke, K. U.; Herranz, J.; Gasteiger, H. A.; Piana, M. Reactivity of the Ionic Liquid Pyr_{14}TFSI with Superoxide Radicals Generated from KO_2 or by Contact of O_2 with $Li_7Ti_5O_{12}$. *J. Electrochem. Soc.* **2015**, *162*, A905−A914.

(39) Schwenke, K. U.; Meini, S.; Wu, X.; Gasteiger, H. A.; Piana, M. Stability of Superoxide Radicals in Glyme Solvents for Non-Aqueous Li-O2 Battery Electrolytes. *Phys. Chem. Chem. Phys.* **2013**, *15*, 11830−11839.

(40) Gokel, G. W.; Cram, D. J.; Liotta, C. L.; Harris, H. P.; Cook, F. L. Preparation and Purification of 18-Crown-6[1,4,7,10,13,16-Hexaoxacyclooctadecane]. *J. Org. Chem.* **1974**, *39*, 2445−2446.

(41) Sharon, D.; Hirshberg, D.; Afri, M.; Frimer, A. A.; Noked, M.; Aurbach, D. Aprotic Metal-Oxygen Batteries: Recent Findings and Insights. *J. Solid State Electrochem.* **2017**, 1861−1878.

(42) Liu, R. H.; Fu, S. Y.; Zhan, H. Y.; Lucia, L. A. General Spectroscopic Protocol to Obtain the Concentration of the Superoxide Anion Radical. *Ind. Eng. Chem. Res.* **2009**, *48*, 9331−9334.

DOI: 10.1021/acsami.7b18376